

Formation and High Mechanical Strength of Bulk Glassy Alloys in Zr–Al–Co–Cu System

Takeshi Wada^{1,*}, Tao Zhang² and Akihisa Inoue²

¹Graduate School, Tohoku University, Sendai 980-8579, Japan

²Institute of Materials Research, Tohoku University, Sendai 980-8577, Japan

The thermal stability of supercooled liquid in the temperature range before crystallization was examined in $Zr_{55}Al_{45-x-y}Co_xCu_y$ alloys without Ni element and the large supercooled liquid region exceeding 80 K was obtained at the compositions around $Zr_{55}Al_{20}Co_{20}Cu_5$ and $Zr_{55}Al_{15}Co_{7.5}Cu_{22.5}$. By choosing the alloy composition of $Zr_{55}Al_{20}Co_{20}Cu_5$, we have formed bulk glassy alloys in rod and sheet forms by copper mold casting and melt-clamp die forging. The maximum diameter and sheet thickness were 5 mm and 3 mm, respectively. The T_g , ΔT_x and T_g/T_l are 746 K, 84 K and 0.61, respectively, being independent of sample thickness. The bulk alloy sheet exhibits Young's modulus of 92 GPa, elastic elongation limit of 2.1% and high tensile strength of 1960 MPa. These strength values are considerably higher than those for the other Zr-based bulk glassy alloys reported up to date. The synthesis of the new Zr–Al–Co-based bulk glassy alloy with high glass-forming ability, large supercooled liquid region and high tensile strength approaching 2000 MPa is expected to result in a future extension of application fields as a high strength material.

(Received January 14, 2003; Accepted July 14, 2003)

Keywords: bulk glassy alloy, new zirconium base system, glass-forming ability, glass transition, mechanical strength

1. Introduction

Since the first syntheses of bulk glassy alloys in metal-metal alloy systems without any metalloid elements such as Ln-,¹⁾ Mg-²⁾ and Zr-³⁾ based alloys by copper mold casting methods, bulk glassy alloys have been regarded as a new family of bulk metallic alloys, in addition to bulk crystalline metallic alloys which have been used for several thousands years. When much attention is paid to Zr-based alloys, bulk glassy alloys with good mechanical properties and a large supercooled liquid region before crystallization have been formed in Zr–Al–Ni,³⁾ Zr–Al–Ni–Cu⁴⁾ and Zr–(Ti, Nb)–Al–Ni–Cu⁵⁾ systems. It has subsequently been reported that similar bulk glassy alloys with good mechanical properties are formed in the other Zr-based alloy systems such as Zr–Ti–Be–Ni–Cu,⁶⁾ Zr–(Pd, Ta)–Al–Ni–Cu⁷⁾ and Zr–Al–Be–Ni–Cu.⁸⁾ These Zr-based bulk glassy alloys exhibit high tensile fracture strength of 1500 to 1700 MPa and have been used as sporting goods materials and connection tubes for optical communication fibers.^{9–12)} As is the case for the Zr-based bulk glassy alloys, Ln–Al–(Co, Ni, Cu)¹³⁾ and Pd–Cu–Ni–P¹⁴⁾ bulk glassy alloys possess good mechanical properties as is evidenced from much higher tensile fracture strength as compared with those for the corresponding crystalline alloys. However, there have been no data on bulk glassy alloys exhibiting high tensile fracture strength of 2000 MPa in Zr-, Ln- and Pd-based alloy systems. Very recently, we have found new Cu-^{15–17)} and Ni-¹⁸⁾ based bulk glassy alloys with high tensile fracture strength exceeding 2000 MPa. Simultaneously, we have investigated a dominant factor for achievement of high tensile fracture strength. It has been pointed out that the tensile fracture strength has a strong correlation with glass transition temperature (T_g) and liquidus temperature (T_l) and there is a clear tendency for tensile strength to increase with increasing T_g and T_l .^{15–18)}

Based on the strong correlation, we have searched for a new Zr-based bulk glassy alloy with much higher tensile fracture strength and succeeded in synthesizing Zr–Al–Co ternary bulk glassy alloys with high tensile fracture strength of approximately 2000 MPa.¹⁹⁾ We further examined the possibility of forming a bulk glassy alloy with higher glass-forming ability, higher stability of supercooled liquid and better mechanical properties in Zr–Al–Co–M (M = Fe, Ni or Cu) systems. This paper intends to present the composition dependence of T_g , crystallization temperature (T_x), supercooled liquid region ($\Delta T_x = T_x - T_g$) and reduced glass transition temperature (T_g/T_l) of $Zr_{55}Al_{45-x-y}Co_xCu_y$ glassy alloys and then the thermal stability and mechanical properties of bulk glassy Zr–Al–Co–Cu alloys fabricated on the basis of their composition dependence data.

2. Experimental Procedure

Multi-component $Zr_{55}Al_{45-x-y}Co_xCu_y$ alloy ingots were prepared by arc melting the mixtures of pure metals in an argon atmosphere. The alloy compositions represent the nominal compositions of the mixtures. Glassy alloy ribbons with a cross section of $0.02 \times 1.2 \text{ mm}^2$ were produced by melt spinning. Bulk glassy alloys in rod and sheet forms were produced by copper mold casting and melt-clamp die forging, respectively. The sample dimension was 70 mm in length and 2 to 5 mm in diameter for the cast rods and 2 mm in thickness, 50 mm in width and 70 mm in length for the forged sheets. The glassy phase was identified by X-ray diffraction and optical and transmission electron microscopy (OM and TEM). Thermal stability was examined by differential scanning calorimetry (DSC) at a heating rate of 0.67 K/s. The melting and liquidus temperatures (T_m and T_l) were measured with a differential thermal analyzer (DTA) at a heating and cooling rate of 0.67 K/s. Mechanical properties were measured in tensile and compressive deformation modes with an Instron testing machine. The gauge dimen-

*Graduate Student, Tohoku University.

sions were 1 mm in thickness, 5 mm in width and 15 mm in length for the tensile specimen and 2 mm in diameter and 4 mm in length for the compressive specimen. The strain rate was $5.0 \times 10^{-4} \text{ s}^{-1}$ for the tensile deformation and $2.5 \times 10^{-3} \text{ s}^{-1}$ for the compressive deformation. Fracture surface was examined by scanning electron microscopy (SEM).

3. Results

It was confirmed by X-ray diffraction that a glassy phase without any crystalline peaks was formed in a wide composition range of 0 to 33 at%Al, 0 to 40 at%Co and 0 to 45 at%Cu by melt spinning. Figure 1 shows the DSC curves of the melt-spun $\text{Zr}_{55}\text{Al}_{20}\text{Co}_{25-x}\text{Cu}_x$ glassy alloys. The T_g and T_x decrease gradually in the Cu content range up to 15 at% and then become nearly constant in the higher Cu content range. On the other hand, the $\Delta T_x (= T_x - T_g)$ value is 79 K at 0%Cu, increases slightly to 84 K at 5%Cu and then decreases monotonously with increasing Cu content. Based on these DSC data, the composition dependence of T_g and ΔT_x is shown in Figs. 2(a) and (b), respectively. It is again seen that the T_g increases with increasing Al content and decreasing Cu content and shows a maximum value of 784 K for $\text{Zr}_{55}\text{Al}_{25}\text{Co}_{20}$, while the ΔT_x shows two maximum values of 84 K for $\text{Zr}_{55}\text{Al}_{20}\text{Co}_{20}\text{Cu}_5$ and 105 K for $\text{Zr}_{55}\text{Al}_{15}\text{Co}_{7.5}\text{Cu}_{22.5}$. It is clearly seen that the optimum Al content at which the largest ΔT_x value is obtained increases to 20 at% from the 15 at%Al for the Zr–Co–based alloys. Consequently, the two maximum ΔT_x values seem to reflect the difference in the optimum Al contents between Zr–Co– and Zr–Cu–based glassy alloys. It is noticed that the addition of 5 at%Cu to Zr–Al–Co ternary alloys causes an increase in the ΔT_x value. It is therefore concluded that the highest stability of the supercooled liquid region which is evidenced from the largest ΔT_x is obtained for $\text{Zr}_{55}\text{Al}_{20}\text{Co}_{20}\text{Cu}_5$.

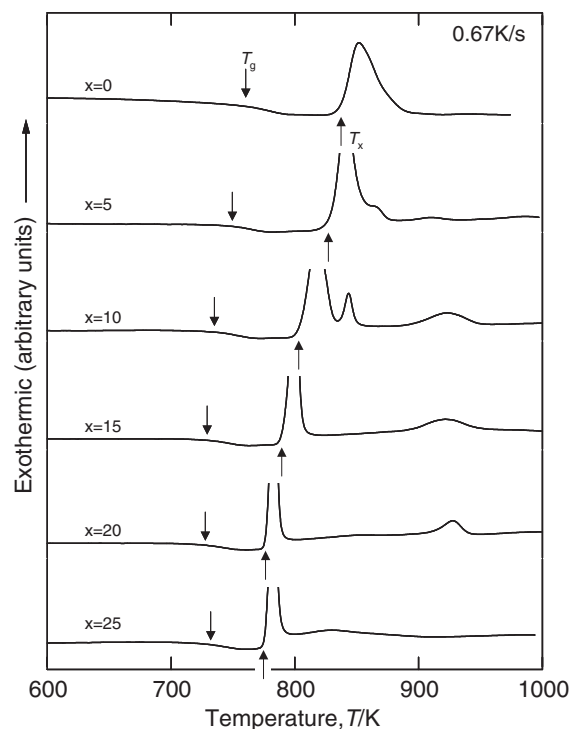


Fig. 1 DSC curves of melt-spun $\text{Zr}_{55}\text{Al}_{20}\text{Co}_{25-x}\text{Cu}_x$ glassy alloys.

Figure 3 shows X-ray diffraction patterns of the cast $\text{Zr}_{55}\text{Al}_{20}\text{Co}_{20}\text{Cu}_5$ samples in a rod form of 3 and 5 mm in diameter and in a sheet form of 2 mm in thickness. The patterns consist only of a broad peak with a wave vector of 25.9 nm^{-1} for all the samples and no appreciable crystalline peak is observed. We have also confirmed the absence of appreciable crystalline phases in the optical micrographs and TEM images of the transverse cross section of the rod and sheet samples. Figure 4 shows DSC curves of the bulk glassy samples in the rod and sheet forms, together with the data of

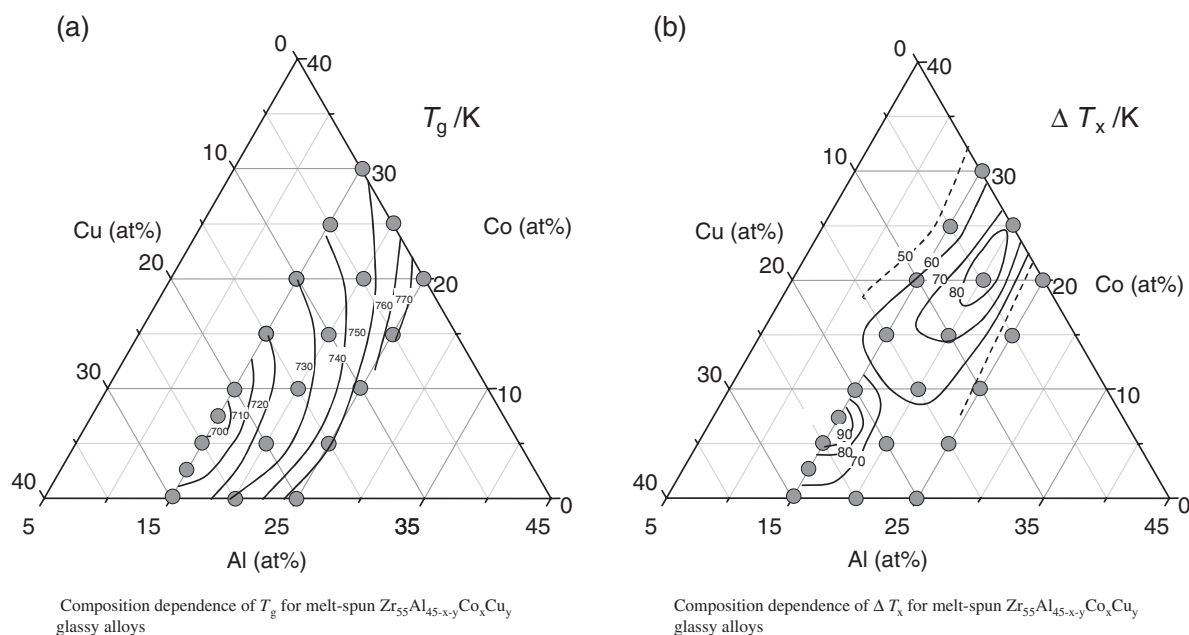


Fig. 2 Composition dependence of T_g and ΔT_x for melt-spun $\text{Zr}_{55}\text{Al}_{45-x-y}\text{Co}_x\text{Cu}_y$ glassy alloys.

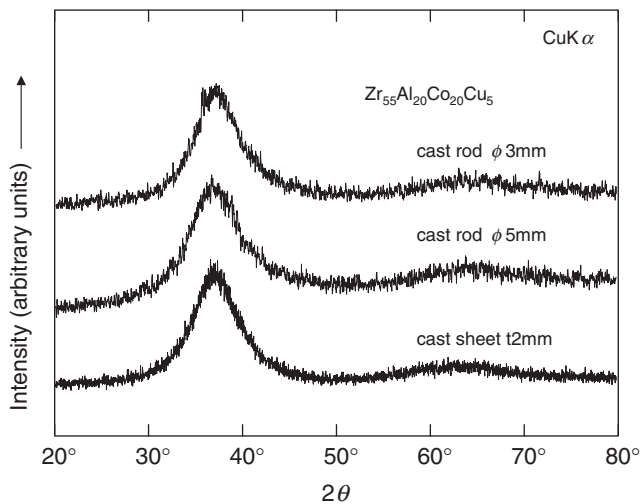


Fig. 3 X-ray diffraction patterns of a $Zr_{55}Al_{20}Co_{20}Cu_5$ alloy in a rod form of 3 and 5 mm in diameter and a sheet form of 2 mm in thickness.

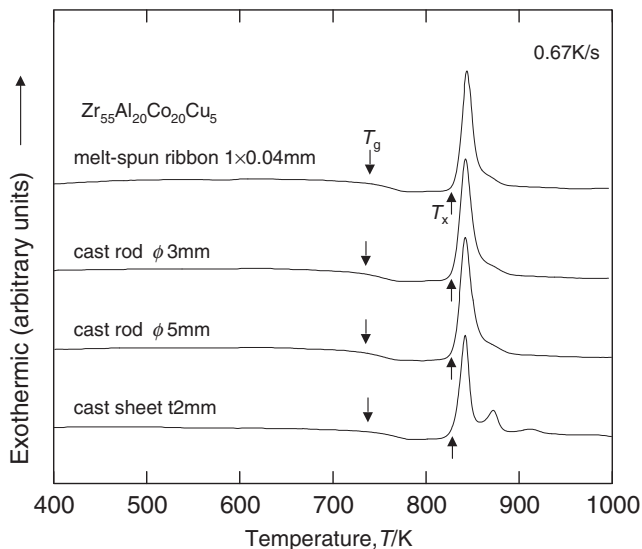


Fig. 4 DSC curves of the glassy $Zr_{55}Al_{20}Co_{20}Cu_5$ alloy in the rod and sheet forms.

the corresponding melt-spun glassy ribbon. All of the DSC curves show nearly the same endothermic and exothermic reactions, *i.e.*, the glass transition, followed by a large supercooled liquid region and then main exothermic peak due to crystallization. The feature of the DSC curves is almost independent of sample thickness. The T_g and T_x are 746 and 830 K, respectively, and the ΔT_x is as large as 84 K which is comparable to those (70 to 127 K)⁴⁾ for Zr–Al–Ni–Cu glassy alloys. With the aim of determining the reduced glass transition temperature (T_g/T_1), we measured the T_1 value by DTA. As shown for the DTA curve in Fig. 5, the alloy solidifies through slightly divided two-stage exothermic reactions and the T_1 is determined as 1220 K. The resulting T_g/T_1 is evaluated to be 0.61 which is high enough to form a bulk glassy alloy by copper mold casting, being consistent with the present results. The DTA data also imply that the elimination of the low intensity exothermic peak causes a significant decrease in T_1 , leading to an increase of T_g/T_1 .

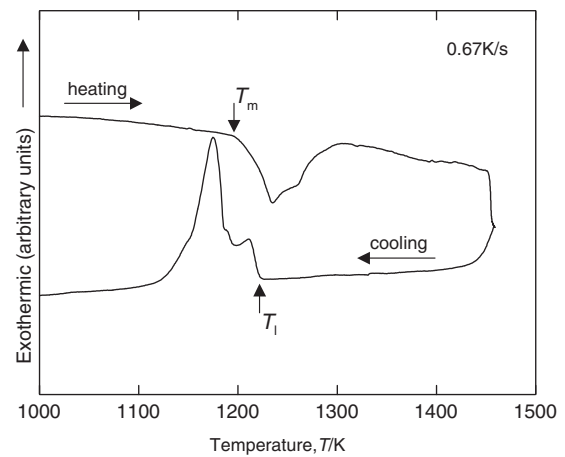


Fig. 5 DTA curve of a $Zr_{55}Al_{20}Co_{20}Cu_5$ alloy prepared by arc melting.

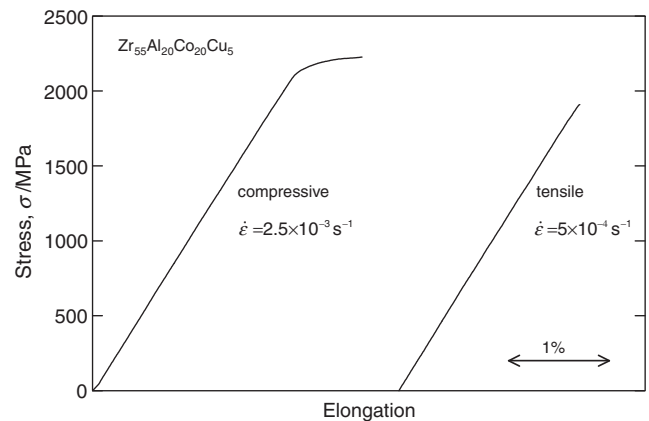


Fig. 6 Stress-elongation curves in tensile and compressive deformation modes for the glassy $Zr_{55}Al_{20}Co_{20}Cu_5$ alloy in a rod form of 2 mm in diameter and a sheet form of 2 mm in thickness.

Figure 6 shows stress-elongation curves of the bulk glassy $Zr_{55}Al_{20}Co_{20}Cu_5$ samples in rod and sheet forms under tensile and compressive deformation modes. No distinct plastic elongation is seen in the tensile stress-elongation curve, but the compressive stress-elongation curve shows a distinct plastic elongation of about 0.6% before final fracture. The Young's modulus (E), elastic elongation limit (ϵ_E), tensile fracture strength ($\sigma_{t,f}$), compressive fracture strength ($\sigma_{c,f}$) and total fracture elongation including elastic elongation (ϵ_f) are 92 GPa, 2.1%, 1960 MPa, 2200 MPa and 2.7%, respectively. It is noticed that the tensile fracture strength reaches 1960 MPa which is considerably higher than those (1500 to 1700 MPa)^{9–12)} for the previously reported Zr-based bulk glassy alloys of Zr–Al–Ni–Cu, Zr–(Ti, Nb, Pd)–Al–Ni–Cu and Zr–Ti–Ni–Cu–Be systems. The fracture under the tensile or compressive deformation mode occurs along a maximum shear stress plane which is declined by about 45 degrees to the direction of applied load and the fracture surface consists mainly of a well-developed vein pattern, as exemplified for the tensile fracture sheet in Fig. 7. The feature of the fracture mode agrees well with those for the other Zr-based bulk glassy alloys.

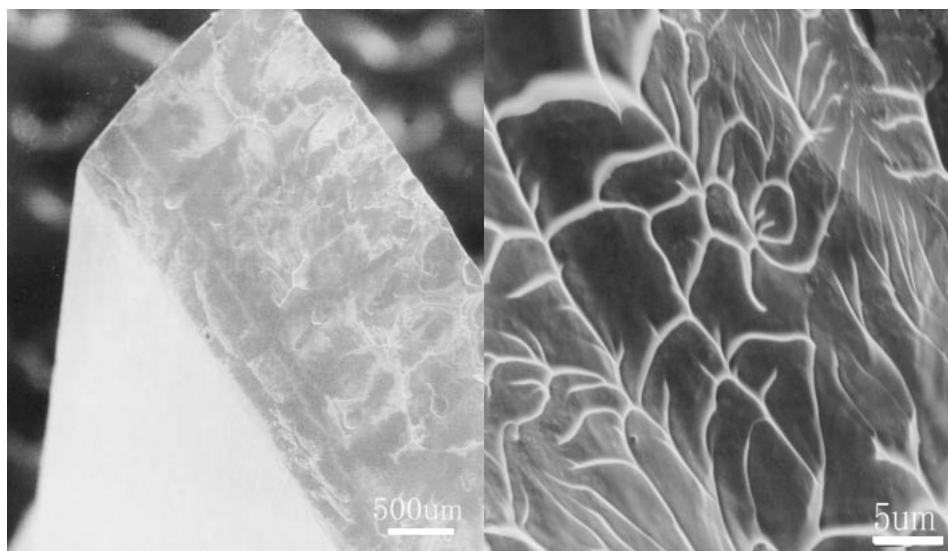


Fig. 7 Fracture surface of the glassy $Zr_{55}Al_{20}Co_{20}Cu_5$ alloy sheet subjected to fracture in a uniaxial tensile deformation mode.

4. Discussion

4.1 High glass-forming ability

As described in section 1, a number of bulk glassy alloys have been synthesized in Zr-based alloy systems. The alloy systems can be classified into two groups of Zr–Al–Ni–Cu type including Ti, Nb, Ta and Pd as additional elements and Zr–Ti–Ni–Cu–Be type.^{9–12} There have been no data on the formation of bulk glassy alloys in Zr–Al–Co base system and the Al content in the previously reported Zr–Al–Ni–Cu bulk glassy alloys is usually in the range from 5 to 15 at%. The higher Al content of 20 at% is another feature of alloy composition for the present Zr-based alloy. Considering that the maximum sample diameter of the $Zr_{55}Al_{20}Co_{20}Cu_5$ glassy alloy is above 5 mm in the case of the copper mold casting method, the glass-forming ability is concluded to be comparable to those for the Zr–Al–Ni–Cu and Zr–(Ti, Nb, Pd)–Ni–Cu systems. We consider the reason for the high glass-forming ability of the new Zr–Al–Co base alloy. It is thought that the base components in the present alloy are the three elements of Zr, Al and Co, though a small amount of Cu (5 at%) is included. It is known that all bulk glassy alloys in metal-metal type system have the following empirical component rules, *i.e.*, (1) multi-component consisting of more than three elements, (2) significant difference in atomic size ratios above 12% among the main three constituent elements, and (3) suitable negative heats of mixing among the main elements.^{9–12} The atomic size ratio is 1.12 for Zr/Al, 1.14 for Al/Co and 1.28 for Zr/Co,²⁰ and the heat of mixing is -44 kJ/mol for Zr–Al pair, -19 kJ/mol for Al–Co pair and -41 kJ/mol for Zr–Co pair.²¹ These data clearly indicate that the Zr–Al–Co base alloy satisfies the above-described component rules for formation of bulk glassy alloys as well as for stabilization of supercooled liquid. It has previously been reported that the bulk glassy alloys with the component rules can have a unique glassy structure with three features of (1) a higher degree of dense random packing state, (2) new local atomic configurations, and (3) long-range homogeneity with attractive interaction.¹¹ It is reasonably

interpreted that the glassy alloy with such structural features can have a highly stable supercooled liquid state through high resistance against atomic rearrangements on a long range scale for the progress of crystallization.

We further discuss the reason why the best alloy composition for high glass-forming ability lies around $Zr_{55}Al_{20}Co_{20}Cu_5$. As shown in Figs. 1 and 5, the DSC curve of the $Zr_{55}Al_{20}Co_{20}Cu_5$ alloy indicates that the crystallization occurs through a nearly single-stage exothermic peak and the solidification from the supercooled liquid also occurs through a low-intensity endothermic peak closely followed by a high-intensity peak. These thermal data suggest that the eutectic point lies in the vicinity of $Zr_{55}Al_{20}Co_{20}Cu_5$. The high reduced glass transition temperature (T_g/T_1) resulting from low T_1 for $Zr_{55}Al_{20}Co_{20}Cu_5$ alloy is presumed to be the origin of the high glass-forming ability at the limited composition in the multi-component alloy system with the three component rules.

4.2 High tensile strength

It is shown in Fig. 6 that the tensile and compressive fracture strength values of the $Zr_{55}Al_{20}Co_{20}Cu_5$ alloy are 1960 MPa and 2200 MPa, respectively. It is noticed that these strength values are much higher than those (1500 to 1800 MPa) for the previously reported Zr-based bulk glassy alloys in Zr–Al–Ni–Cu, Zr–(Ti, Nb, Pd)–Al–Ni–Cu and Zr–Ti–Ni–Cu–Be systems.^{10–13} We discuss the reason for the higher tensile and compressive strength values of the present Zr–Al–Co–Cu bulk glassy alloy. It has been pointed out that the tensile strength has a good linear relation with Young's modulus, T_g and liquidus temperature (T_l) for bulk glassy alloys.^{16,22} The Young's modulus, T_g and T_l of the present Zr-based alloy are 92 GPa, 746 K and 1220 K, respectively, being considerably higher than those (89 to 90 GPa, 690 K and 1113 K) for the other Zr-based bulk glassy alloys. It is therefore concluded that the bonding force among the constituent elements in the Zr–Al–Co–Cu glassy alloy is stronger than that for the other Zr-based glassy alloys. Considering the difference in the alloy components in these

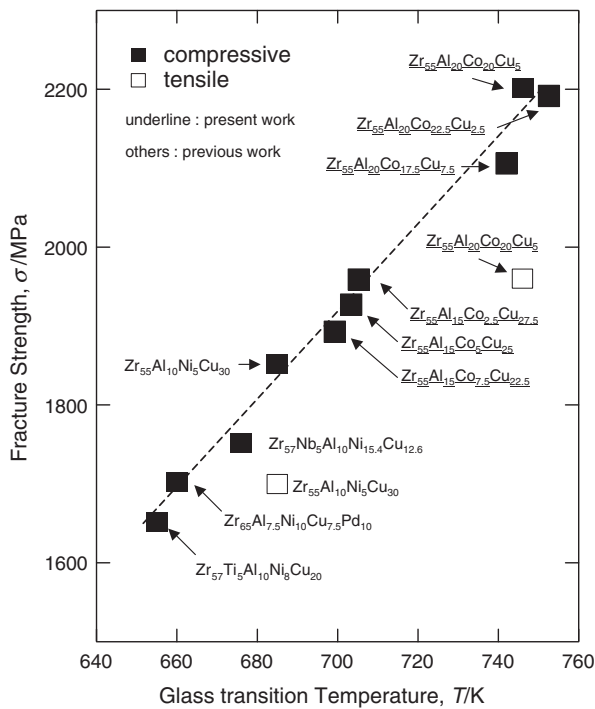


Fig. 8 Relation between tensile or compressive fracture strength and the glass transition temperature for various Zr-based bulk glassy alloys.

Zr-based glassy alloys, the stronger bonding force for the present alloy seems to be mainly attributed to the following two reasons, *i.e.*, (1) the increase in the bonding numbers of Zr–Al, Co–Al and Cu–Al pairs resulting from the higher Al content (20 at%), and (2) the larger average negative heats of mixing (–19 to –41 kJ/mol) for Zr–Co and Al–Co pairs than those (–1 to –49 kJ/mol) for Zr–Ni, Zr–Cu, Al–Ni and Al–Cu pairs.²¹⁾

Figure 8 summarizes the relation between σ_f and T_g for $Zr_{55}Al_{20}Co_{20-x}Cu_{5+x}$ and $Zr_{55}Al_{15}Co_{7.5+y}Cu_{22.5-y}$ ($x = \pm 2.5$, $y = \pm 2.5$) including the optimal composition ($x = 0$, $y = 0$) together with the data for the previously reported Zr-based alloys. A good linear relation between σ_f and T_g was recognized in the Zr–Al–Co–Cu alloys and the Zr-based alloys reported previously. It is again noticed in Fig. 8 that the fracture strength values of $Zr_{55}Al_{20}Co_{17.5-22.5}Cu_{2.5-7.5}$ alloys are considerably higher than those of $Zr_{55}Al_{15}Co_{2.5-7.5}Cu_{22.5-27.5}$ alloys. We further discuss the reason for the significant difference in the fracture strength between the two alloy groups, though their components are just the same. When the atomic configurations in the glassy alloys are assumed to be completely random state, the existing ratios of the solute elements around one Zr atom in the nearest neighbor site are 0.36 for Al, 0.36 for Co and 0.09 for Cu in the Co-rich $Zr_{55}Al_{20}Co_{20}Cu_5$ alloy and 0.27 for Al, 0.13 for Co and 0.41 for Cu in Cu-rich $Zr_{55}Al_{15}Co_{7.5}Cu_{22.5}$ alloy. Consequently the former alloy includes much larger number of Zr–Al and Zr–Co atomic pairs with larger negative heats of mixing, leading to the higher mechanical strength.

4.3 Difference in the fracture strength under tensile and compressive deformation modes

As shown in Fig. 8, the tensile strength values of the Zr–Al–Ni–Cu and Zr–Al–Co–Cu bulk glassy alloys are about 10% lower than the compressive strength values. The difference seems to originate mainly from the following two factors, *i.e.*, (1) the final fracture in the compressive deformation mode always occurs accompanying distinct plastic elongation, while the tensile specimen fractures without distinct plastic elongation, and (2) the specimen for the tensile test was prepared by mechanical cutting leading to the elimination of the surface region with compressive residual stress in the cast sheet alloy. On the other hand, the compressive specimen keeps the original lateral surface of the cast rod alloy, even though the top and bottom surfaces are prepared by mechanical cutting. Thus, the elimination of the surface region with residual compressive stress component in the cast alloy may be the origin for the decrease in fracture strength through the loss of plastic elongation.

5. Summary

The largest supercooled liquid region in Zr–Al–Co-based alloys was found to be obtained for $Zr_{55}Al_{20}Co_{20}Cu_5$. The T_g , ΔT_x and T_g/T_l values were 746 K, 84 K and 0.61, respectively. By choosing the alloy composition with the largest ΔT_x , we produced a new Zr-based bulk glassy alloy with a diameter up to 5 mm by copper mold casting. The T_g , ΔT_x and T_g/T_l of the bulk glassy alloy rod with a diameter of 5 mm were just the same as those for the corresponding melt-spun ribbon alloy. The Young's modulus, elastic elongation limit, tensile fracture strength, compressive fracture strength and compressive plastic elongation of the cast bulk glassy alloy rod are 92 GPa, 2.1%, 1960 MPa, 2200 MPa and 0.6%, respectively. It is noticed that the tensile fracture strength is considerably higher than those (1500 to 1700 MPa) for the other Zr-based bulk glassy alloys. The higher strength combined with high glass-forming ability and large supercooled liquid region for the new Zr-based alloys without Ni element is promising as a new type of high-strength bulk glassy alloy.

REFERENCES

- 1) A. Inoue, T. Zhang and T. Masumoto: Mater. Trans. JIM **30** (1989) 965–972.
- 2) A. Inoue, K. Ohtera, K. Kita and T. Masumoto: Jpn. J. Appl. Phys. **27** (1989) L2258–L2261.
- 3) A. Inoue, T. Zhang and T. Masumoto: Mater. Trans. JIM **31** (1990) 177–183.
- 4) T. Zhang, A. Inoue and T. Masumoto: Mater. Trans. JIM **32** (1991) 1005–1010.
- 5) A. Inoue, T. Shibata and T. Zhang: Mater. Trans. JIM **36** (1995) 1420–1426.
- 6) A. Pecker and W. L. Johnson: Appl. Phys. Lett. **63** (1993) 2342–2344.
- 7) A. Inoue, Y. Yokoyama, Y. Shinohara and T. Masumoto: Mater. Trans. JIM **35** (1994) 923–926.
- 8) A. Inoue, T. Zhang, N. Nishiyama, K. Ohba and T. Masumoto: Mater. Trans. JIM **34** (1993) 1234–1237.
- 9) A. Inoue: Mater. Trans. JIM **36** (1995) 866–875.
- 10) A. Inoue: Acta Mater. **48** (2000) 279–306.
- 11) A. Inoue: Mater. Sci. Eng. **A304–306** (2001) 1–10.
- 12) *Supercooled Liquid, Bulk Glassy, and Nanocrystalline State of Alloys*,

- ed. by A. Inoue, A. R. Yavari, W. L. Johnson and R. H. Dauskardt (MRS, Warrendale, 2001) pp. L12.13.1-L12.13.6.
- 13) A. Inoue, T. Nakamura, T. Sugita, T. Zhang and T. Masumoto: *Mater. Trans. JIM* **34** (1993) 351–358.
- 14) A. Inoue, N. Nishiyama and T. Masuda: *Mater. Trans. JIM* **37** (1996) 181–184.
- 15) A. Inoue, W. Zhang, T. Zhang and K. Kurosaka: *Acta Mater.* **49** (2001) 2645–2652.
- 16) A. Inoue, W. Zhang, T. Zhang and K. Kurosaka: *Mater. Trans.* **42** (2001) 1142–1145.
- 17) A. Inoue, W. Zhang, T. Zhang and K. Kurosaka: *Mater. Trans.* **42** (2001) 1149–1151.
- 18) A. Inoue, T. Zhang, K. Kurosaka and W. Zhang: *Mater. Trans.* **42** (2001) 1800–1804.
- 19) T. Zhang and A. Inoue: *Mater. Trans.* **43** (2002) 267–270.
- 20) *Metal Databook*, ed by Japan Inst. Metals, (Maruzen, Tokyo, 1983) pp. 8
- 21) F. R. de Boer, R. Boom, W. C. M. Mattens, A. R. Miedema and A. K. Niessen: *Cohesion in Metals, Transition Metal Alloys* (North-Holland, Amsterdam, 1988).
- 22) H. S. Chen: *Rep. Prog. Phys.* **43** (1980) 353–432.